SANDIA REPORT

SAND99–0924
Unlimited Release
Printed April 1999

Advanced Concepts for High-Power VCSELs and 2-Dimensional VCSEL Arrays

Kent D. Choquette, R. Hadley, W. W. Chow, A. A. Allerman, K. M. Geib, A. Mar, and H. Q. Hou

Prepared by
Sandia National Laboratories
Albuquerque, New Mexico 87185 and Livermore, California 94550

Sandia is a multiprogram laboratory operated by Sandia Corporation, a Lockheed Martin Company, for the United States Department of Energy under Contract DE-AC04-94AL85000.

Sandia National Laboratories

Issued by Sandia National Laboratories, operated for the United States Department of Energy by Sandia Corporation.

Available to DOE and DOE contractors from
Office of Scientific and Technical Information
P.O. Box 62
Oak Ridge, TN 37831

Prices available from (703) 605-6000
Web site: http://www.ntis.gov/ordering.htm

Available to the public from
National Technical Information Service
U.S. Department of Commerce
5285 Port Royal Rd
Springfield, VA 22161

NTIS price codes
Printed copy: A03
Microfiche copy: A01

SAND99-0924
Unlimited Release
Printed April 1999

Advanced Concepts for High-Power VCSELs and 2-Dimensional VCSEL Arrays

Kent D. Choquette, R. Hadley, W. W. Chow,
A. A. Allerman, K. M. Geib, A. Mar, and H. Q. Hou
Photonics Research Department
Center for Compound Semiconductor Science and Technology
Sandia National Laboratories
P.O. Box 5800
Albuquerque, NM 87185-0603

Abstract

We have developed high power vertical cavity surface emitting lasers (VCSELs) for multimode or single mode operation. We have characterized new cavity designs for individual lasers and 2-dimensional VCSEL arrays to maximize output power. Using broad area high power VCSELs under pulsed excitation, we have demonstrated the triggering of a photoconductive semiconductor switch (PCSS) with a VCSEL. We also have developed designs for high output power in a single mode. The first approach is to engineer the oxide aperture profile to influence the optical confinement and thus modal properties. A second approach focuses on "leaky-mode" concepts using lateral modification of the cavity resonance to provide the lateral refractive index difference. To this end, we have developed a regrowth process to fabricate single mode VCSELs. The overall objective of this work was to develop high-power single mode or multimode sources appropriate for many applications leveraging the many inherent advantages of VCSELs..

Acknowledgements:

The authors are indebted to a several of researchers formerly and presently at Sandia, including: B. E. Hammons, K. L. Lear, D. Serkland, and J. Nevers.

This work was supported by the United States Department of Energy under Contract DE-AC04-94AL85000. Sandia is a multiprogram laboratory operated by Sandia Corporation for the United States Department of Energy.

ADVANCED CONCEPTS FOR HIGH-POWER VCSELS AND 2-DIMENSIONAL VCSEL ARRAYS

Table of Contents

1. INTRODUCTION 1

2. MULTIMODE VCSEL OUTPUT 1

2.1. INDIVIDUAL VCSELS 2

2.2. VCSEL ARRAYS 6

3. SINGLE MODE VCSEL OUTPUT 9

3.1. OXIDE APERTURE DESIGNS 10

3.2. LEAKY MODE DESIGNS 14

4. SUMMARY 18

ADVANCED CONCEPTS FOR HIGH-POWER VCSELS AND 2-DIMENSIONAL VCSEL ARRAYS

Table of Figures

Figure 1. Effects of dopant profile on VCSEL efficiency. 3
Figure 2. Effects of output mirror reflectivity on VCSEL efficiency..... 3
Figure 3. Scaling properties of threshold current and maximum power. 4
Figure 4. Light output characteristics of pulsed VCSEL. 5
Figure 5. Pulsed output of selectively oxidized VCSEL. 6
Figure 6. 8x8 individually addressed VCSEL array. 7
Figure 7. Light output from array VCSEL and maximum power. 7
Figure 8. Thermal cross talk effects in 8x8 VCSEL array. 8
Figure 9. CW light output characteristics for 8x8 VCSEL array. 8
Figure 10. TEM image of quarterwave thick oxide..... 10
Figure 11. TEM image of thick tapered oxide. 11
Figure 12. TEM image of thin oxide. 11
Figure 13. Near field mode width versus aperture size..... 12
Figure 14. Maximum single mode power versus aperture size..... 13
Figure 15. Design plot for leaky mode VCSELs. 14
Figure 16. Leaky mode VCSEL utilizing transverse resonance modification.... 15
Figure 17. Scanning electron microscope image of leaky mode VCSEL. 15
Figure 18. Light output and lasing spectrum for VCSEL with.Δn=0.06 16
Figure 19. Light output and lasing spectrum for VCSEL with Δn=0.03 17

1. Introduction

High power laser sources are in increasingly greater demand for both commercial as well as defense applications. Examples of the latter are laser targeting, laser triggering, power transmission, and free-space communications. Although vertical cavity surface emitting lasers (VCSELs) have become established as low power high efficiency devices, virtually no work has been performed to exploit these lasers for possible pulsed high-power applications. Moreover, high power single mode VCSELs are desired for many applications. In this project we have explored and characterized designs for high power VCSELs with multimode and single mode output.

VCSEL heterostructure designs for high power multimode operation, particularly pulsed high power, are generally not appropriate for efficient CW operation. Thus consideration of pulsed high power VCSELs could open up an entirely new opportunity for VCSEL applications. We characterized the effects of cavity design (mirror reflectivity, doping distribution, and cross section area) for high power pulsed operation. We have also examined 2-dimensional VCSEL arrays to achieve high multimode output.

Conventional approaches to single mode operation of edge emitting lasers has relied on leaky mode structures. This has been shown to be effective in structurally enhancing mode selectivity at high single-mode output powers in edge-emitting lasers and generally utilize a higher-index material surrounding the laser cavity that leads to index anti-guiding. Analogous designs in VCSELs have proved to be rather elusive due to stringent demands on fabrication. Specifically, edge emitting leaky-mode arrays have relied on epitaxial regrowth to achieve lateral refractive index modifications. This is difficult in VCSELs due to the prevalence of tenacious native oxides that preclude regrowth.

We have considered two approaches for achieving high power single mode VCSELs. First, we have designed novel oxide apertures to promote modal discrimination in the index-guided cavity. Secondly, we have pursued leaky mode designs for single mode operation. We have employed transverse cavity resonance modification to achieve leaky mode characteristics, based on recent Sandia modeling. To obtain a lateral variation in the cavity resonance we developed a VCSEL regrowth technique which uses MOVPE overgrowth of upper the mirror distributed Bragg reflector (DBR) on a patterned optical cavity.

2. Multimode VCSEL Output

For many high power laser applications, multimode operation is permissible. Although VCSELs are typically multimode lasers, high power operation is

problematic. This is because of the ultra-small active volume inherent to a VCSEL. For conventional edge emitting lasers it is straightforward to increase to output power by increasing the length of the laser bar. This approach is very difficult within a VCSEL, since increasing the cavity length leads to excessive optical loss. One aspect that can be adjusted in a VCSEL is the output coupling; by trading off higher threshold current, one can obtain higher slope efficiency and thus high power operation. In addition, the dopant distribution within the mirrors will influence the laser slope efficiency. The VCSEL cross section area can be increased to provide greater output power, but only up to a point. There is an upper limit to the practical VCSEL size due to current transport and thermal issues. This naturally leads to the use of 2-dimensional VCSEL arrays to increase the power output.

2.1. Individual VCSELs

In this section, we consider the effects of the cavity design (output DBR reflectivity and dopant distribution) and the cavity cross section area on high power operation. We also demonstrate high power pulsed operation of VCSELs and their application to trigger high power photoconductive switches.

2.1.1. Cavity Design

High efficiency VCSELs are attractive for emerging applications, such as optical data links or free space interconnects, since high efficiency implies relaxed power budgets and lower parasitic thermal dissipation. High power operation requires high external quantum efficiency, η_{ex}. Here we show the effects of doping concentration and reflectivity of the mirror on the efficiency of 850 and 780 nm oxide-confined VCSELs, the results of which are important for design of high power VCSELs.

The VCSEL wafers are grown by MOVPE, where the 850 (780) nm VCSELs use five quantum wells of GaAs (AlGaAs) embedded within a one wavelength thick optical cavity. For the doping experiments, the 850nm VCSELs have 22(33) top C-doped (bottom Si-doped) DBR periods. The doping in the optical cavity is held constant, while the doping in the first 3 periods next to the cavity and the remaining outer periods of each DBR are varied between 0.5 and $4x10^{18}$ cm^{-3}. For the reflectivity experiments, the mirror doping is held constant, while the number of periods in the top output DBR is varied.

Figure 1 shows that the VCSEL external quantum efficiency monotonically increases as the doping level in the various regions of the p- and n-type DBR are decreased. It has been previously recognized that reduced doping near the optical cavity can improve VCSEL performance, due to penetration of the longitudinal

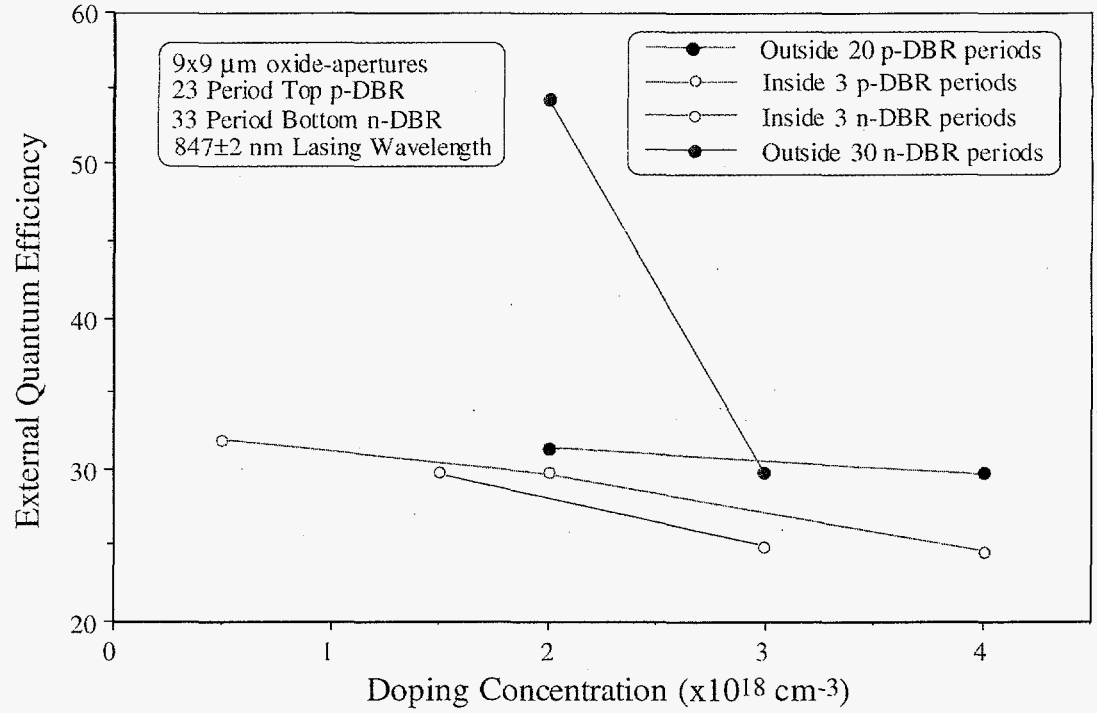

Figure 1. Effects of dopant profile on VCSEL efficiency.

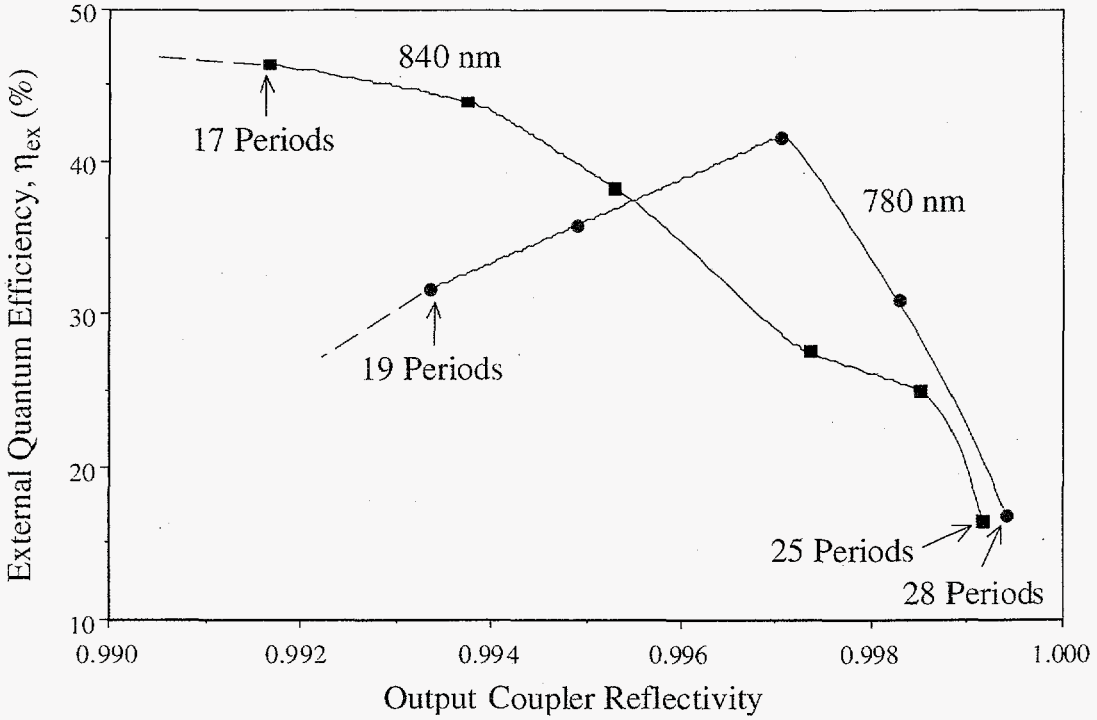

Figure 2. Effects of output mirror reflectivity on VCSEL efficiency.

mode in the mirror and the accompanying optical absorption. However, Fig. 1 also shows that the doping level in the n-DBR has a significant impact. Decreased doping throughout the n-type mirror produces significantly higher quantum efficiency, in spite of the small penetration of the optical fields through the outermost portions of the DBR.

Figure 2 shows the dependence of η_{ex} on the mirror reflectivity for both 850 and 780 nm VCSELs. For large number of DBR periods (high reflectivity), η_{ex} is low due to the small transmission of light through the output DBR. For low number of periods (low reflectivity) η_{ex} is reduced due to increased absorption. Thus as evident for the 780 nm VCSELs in Fig. 2, an optimum output reflectivity exists for high efficiency operation. For the 850nm VCSELs in Fig. 2, the optimum reflectivity is less (less number of periods) than that of the 780nm VCSELs, due to the decreased material gain in AlGaAs as compared to GaAs.

An obvious means to increase the output power from a VCSEL is to increase its cross section area. However, there are limits to the practical size of broad area VCSELs. As shown in Figure 3, the threshold current scales quadratically with the aperture diameter, while the output power increases only linearly with aperture size. Thus the quantum efficiency decreases for sufficiently large aperture area. We have found for continuous wave operation, that aperture areas > 20x20 μm are not practical.

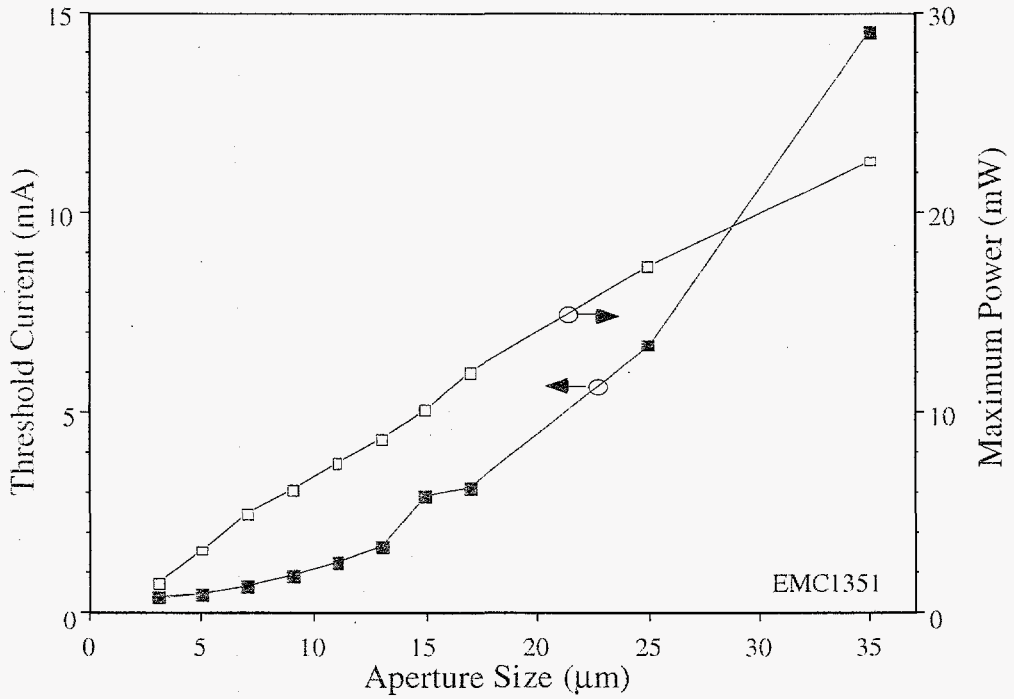

Figure 3. Scaling properties of threshold current and maximum power with aperture size.

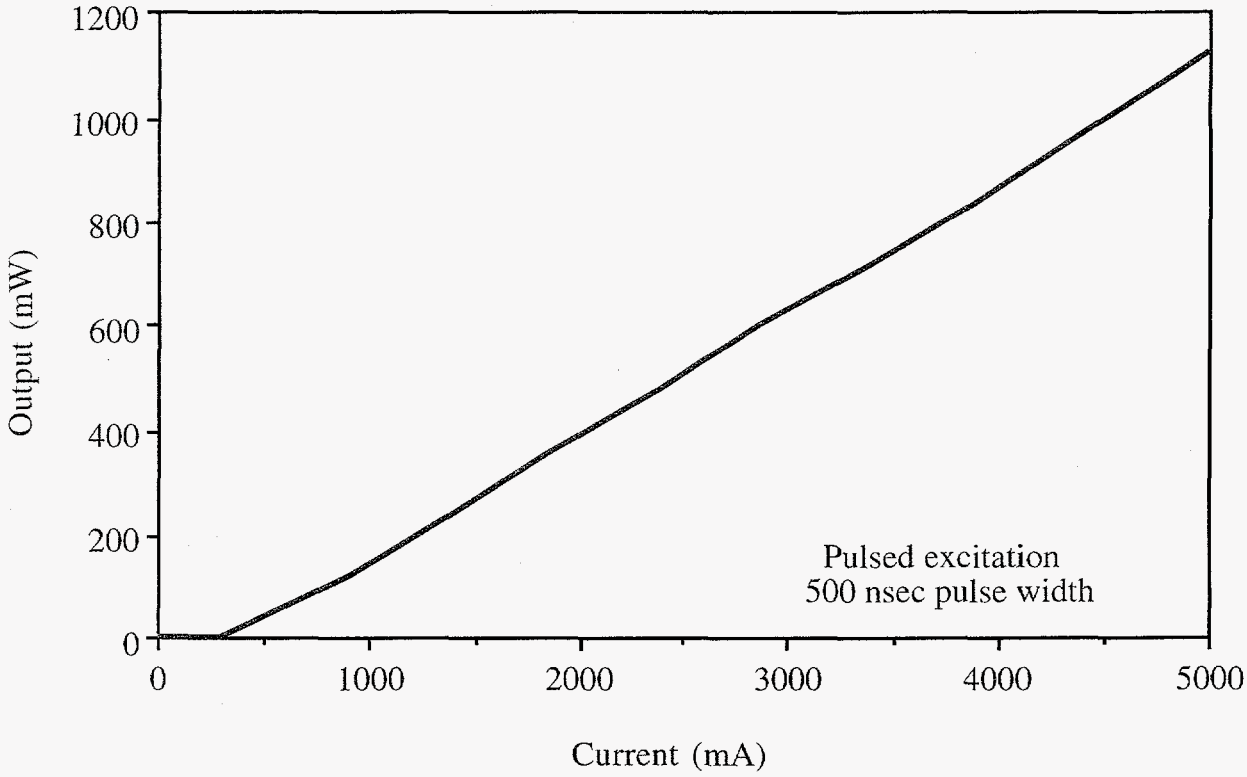

Figure 4. Light output characteristics of pulsed VCSEL.

2.1.2. VCSEL Pulsed Operation

Under pulsed operation, the aperture size considerations become less important for high power VCSEL operation. Figure 4 illustrates the light versus current characteristics of a pulsed broad area VCSEL. As shown in Fig. 4, the maximum pulsed (300 nsec pulse width) output power that has been observed is 1.1 W from a broad area 980 nm VCSEL which emits through the substrate backside. The output power was measurement limited (maximum of 5A), rather than limited by the device.

For reasons of manufacturability, reliability, cost, and packaging, the integration of high-gain, high-power photoconductive semiconductor switches (PCSS) with trigger lasers has important implications for many applications. VCSELs may play an important role in the implementation of such a device due to their advantages of surface normal emission and ease of array fabrication and on-wafer testing. An outstanding issue for VCSEL triggering of PCSS devices has been that of the optical pulse energy required to cause the switch triggering. Previously, the minimum energy that had been observed to achieve switch firing was 13.6 nJ in a 40 μm diameter spot of illumination, at a wavelength of 532 nm. Such energies may be difficult to extract from VCSELs due to their relatively small lasing volumes.

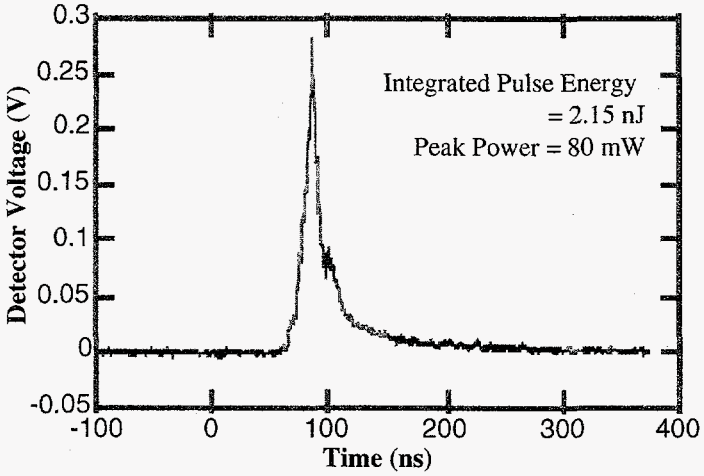

Figure 5. Pulsed output of selectively oxidized VCSEL.

However, we successfully demonstrated the triggering of a PCSS using a VCSEL. As shown in Figure 5, this VCSEL emits pulses of 2.15 nJ energy, and a peak power of 80 mW. These may be underestimated due to the limited bandwidth of the photodetector and oscilloscope used to obtain the measurement. The pulse width of the VCSEL under pulsed operation using a streak camera measurement was found to be 18 psec, which when deconvolved from the system response gives a pulse width of ≈13 psec. The laser has a square emitting aperture of 75 μm width, with a lasing wavelength of 850 nm, and is optimized for high output (as opposed to low threshold) with only 17 mirror pairs forming the output coupling mirror, and an active region containing 5 quantum wells. A high numerical aperture, aberration-free lens was used to image the VCSEL output onto the surface of the switch with nominally unity magnification. The triggered switch has a 1 mm gap and was biased at 3.5 KV, resulting in a current pulse of 43 A upon triggering. The demonstration that a PCSS can be triggered with a single short pulse VCSEL is of importance for PCSS based components such as firing set switches, high speed laser diode array pulsed sources, and low jitter drivers.

2.2. VCSEL Arrays

The compatibility of 2-dimensional array fabrication is an inherent attribute of VCSELs. With recent advances in VCSEL performance afforded by the advent of oxidized current apertures, 2-dimensional (2-D) arrays of individually addressable selectively oxidized vertical cavity surface emitting lasers (VCSELs) have come under scrutiny. High power 2-dimensional VCSEL arrays would be appropriate for such applications as optical data interconnects and transmission, printing, displays, and perhaps even pumping for solid state lasers. An example

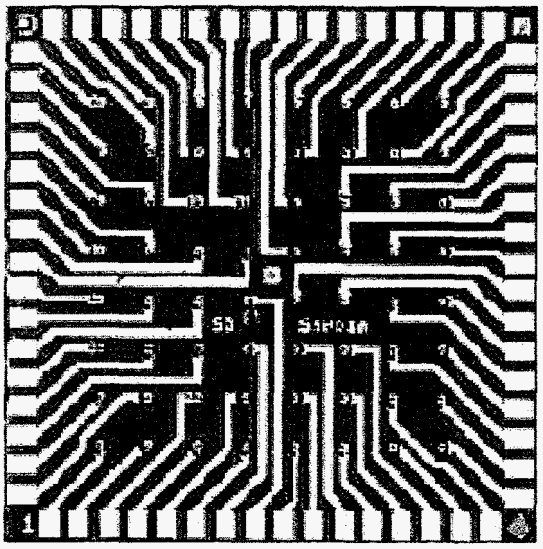

Figure 6. 8x8 individually addressed VCSEL array.

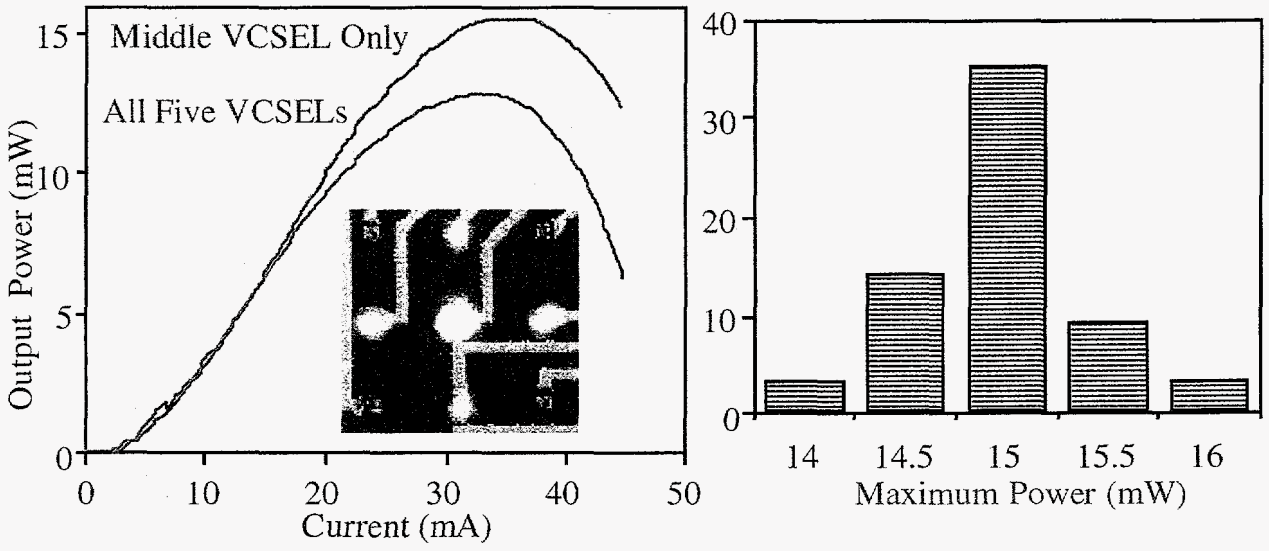

Figure 7. Light output from individual VCSEL in array and maximum power obtained from elements of 8x8 array.

of an 8x8 array in operation is shown in Figure 6. Uniformity of array characteristics such as threshold and operating current is an important consideration, particularly to simplify interfacing the array to microelectronic drive circuitry. Moreover, high power (albeit multimode) emission from each element is desirable, in spite of thermal management problems that may arise. The output power of a single VCSEL scales linearly with aperture size, while the threshold current scales quadratically with aperture size (see Fig. 3). Thus, using multiple high efficiency elements may be better than a single broad area VCSEL. In the following, we consider 8x8 VCSEL arrays for achieving high output power.

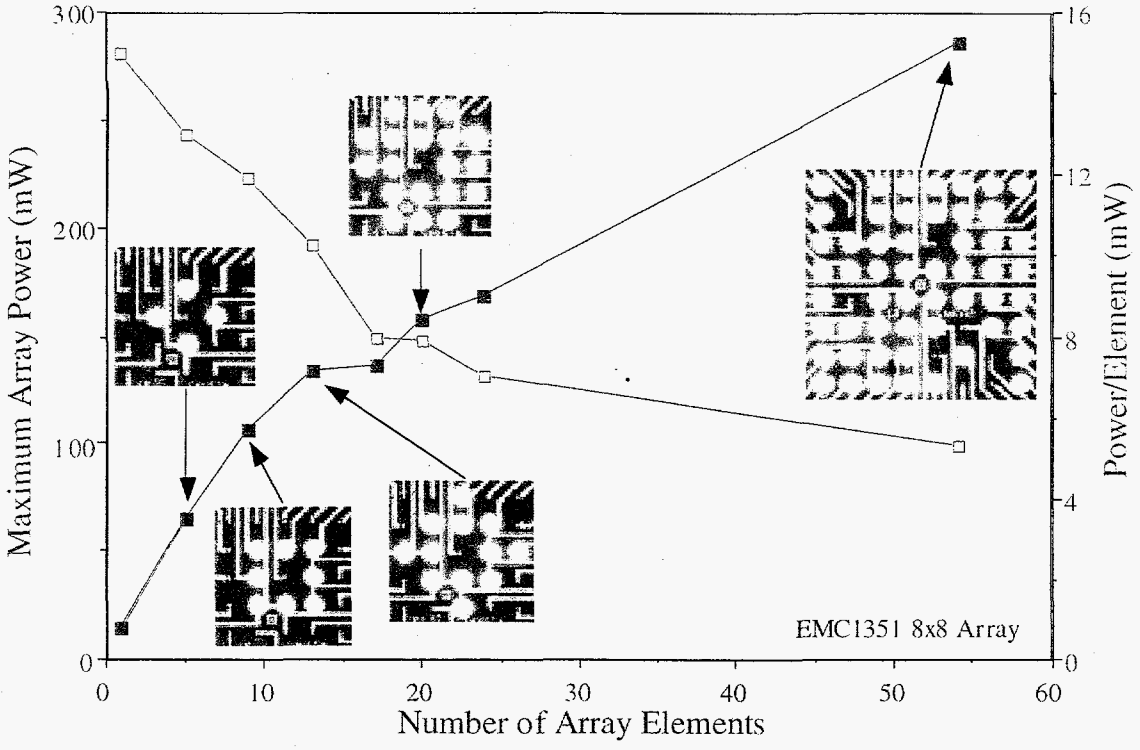

Figure 8. Thermal cross talk effects in 8x8 VCSEL array.

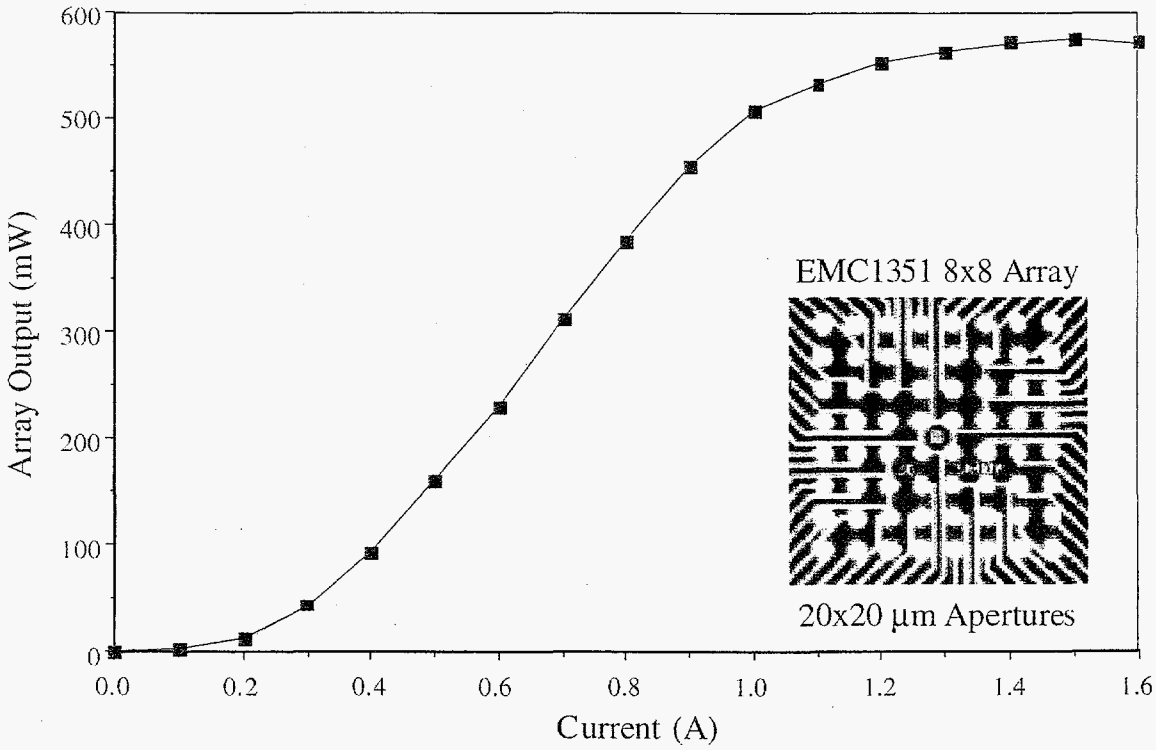

Figure 9. CW light output characteristics for 8x8 VCSEL array.

To achieve high power array operation, we leverage the optimized cavity designs described above. For example, in the 6 DBR periods on each side of the optical cavity the doping profile is decreased to as low as $5x10^{17}$ cm^{-3} for reduced optical absorption (see Figure 1). This design enhances the output power at the expense of relatively higher threshold voltage. Figure 7 shows CW light vs. current (L-I) curves for a typical VCSEL in the array. Each array element he individual average threshold current is 2.5±0.1 mA; the average threshold voltage is 2.66±0.02 V. Figure 7 also illustrates that uniform high output power (average 15.2±0.4 mW) is found for all elements of the 8x8 array.

Thermal issues in 2-dimensional arrays are also important, especially for simultaneous CW operation of multiple elements. In Fig. 7 are shown CW L-I curves arising from the center VCSEL with its four nearest neighbors (see inset) at various operating currents. As apparent in Fig. 7, when all five elements are driven to their maximum output (33 mA), the output from each VCSEL is only reduced from ≈15 to 13 mW. The thermal cross talk between elements is also depicted in Figure 8. As more array elements are turned on, the average power per array VCSEL decreases. Figure 9 shows the CW output power from an 8x8 VCSEL array emitting at 850 nm. The array is packaged into a pin grid array package which is actively cooled. The peak power is nearly 600 mW but is still limited by parasitic heating. Achieving higher output power will require further refinement of the array packaging.

3. Single Mode VCSEL Output

Buried oxide apertures within VCSELs transversely confine both charge carriers and photons. The strong index-guided confinement within selectively oxidized VCSELs produces very little modal discrimination, resulting in multi-mode operation. Decoupling the electrical and optical confinement arising from the oxide apertures will allow tailoring specific VCSEL performance. For example by reducing the transverse optical confinement while maintaining a small current injection aperture, VCSELs which promote a single transverse mode can be fabricated. Moreover, reduction of the transverse confinement will tend to reduce the multi-mode behavior of VCSELs. In addition to confinement, the optical loss for small oxide confined VCSELs is influenced by the thickness, tapering, and position of the apertures. We have developed specific oxide aperture profiles to control the transverse confinement and modal discrimination.

We have also pursued leaky mode designs for single mode VCSEL operation. We have employed transverse cavity resonance modification to achieve leaky mode characteristics, based on recent Sandia modeling. To obtain a lateral variation in the cavity resonance we developed a VCSEL regrowth technique which uses MOVPE overgrowth of upper the mirror distributed Bragg reflector (DBR) on a patterned optical cavity.

3.1. Oxide Aperture Designs

To achieve single mode operation in a selectively oxidized VCSEL, the inherent optical confinement must be reduced and higher order optical modes should be suppressed. A conventional "quarterwave length" thick oxide aperture on each side of the optical cavity is shown in the transmission electron microscope (TEM) image in Figure 10. In the following, we describe oxide aperture designs that have been considered to achieve single mode operation.

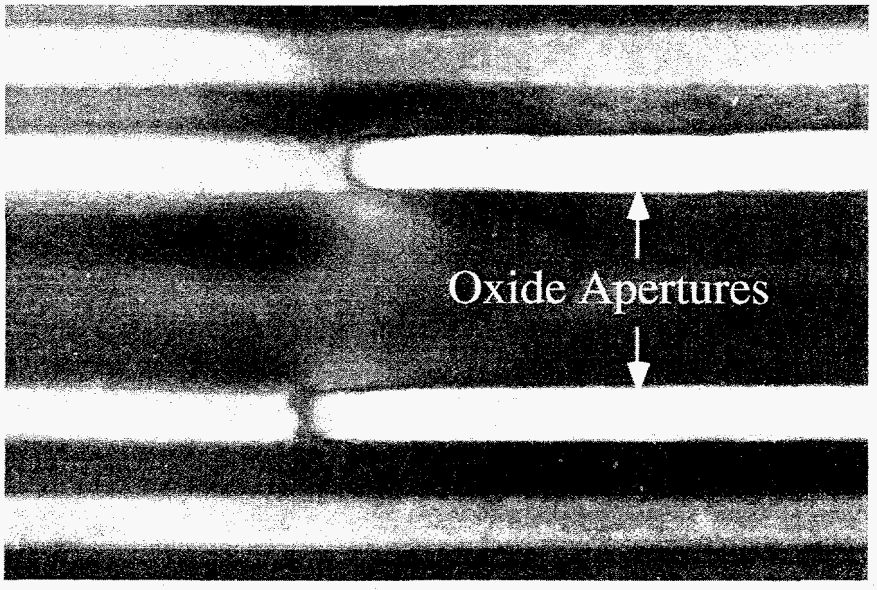

Figure 10. TEM image of quarterwave thick oxide on each side of optical cavity.

3.1.1. Oxide Profile

With better understanding of the wet oxidation of AlGaAs, elaborate buried oxide aperture designs within VCSELs have been pursued. In Figures 11 and 12 we show examples of two transparent oxide apertures considered. For both designs a high Al-content layer is located at a null position of the longitudinal standing wave within a nominally 3/4-wavelength thick layer in the high or low index layer of the first period of the distributed Bragg reflector (DBR) adjacent to the optical cavity. Note that the 3/4-wavelength thick layer provides access to both a longitudinal field null or antinode, while avoiding the complication from the compositional grading between the usual 1/4-wavelength thick high and low index layers of the distributed Bragg reflector.

Nominally 850 nm VCSELs with a 21 period $Al_{0.16}Ga_{0.84}As/Al_{0.92}Ga_{0.08}As$ top DBR mirror were fabricated. The oxide aperture designs shown in Figs. 11 and 12 were included in the first DBR period next to the optical cavity. As shown in

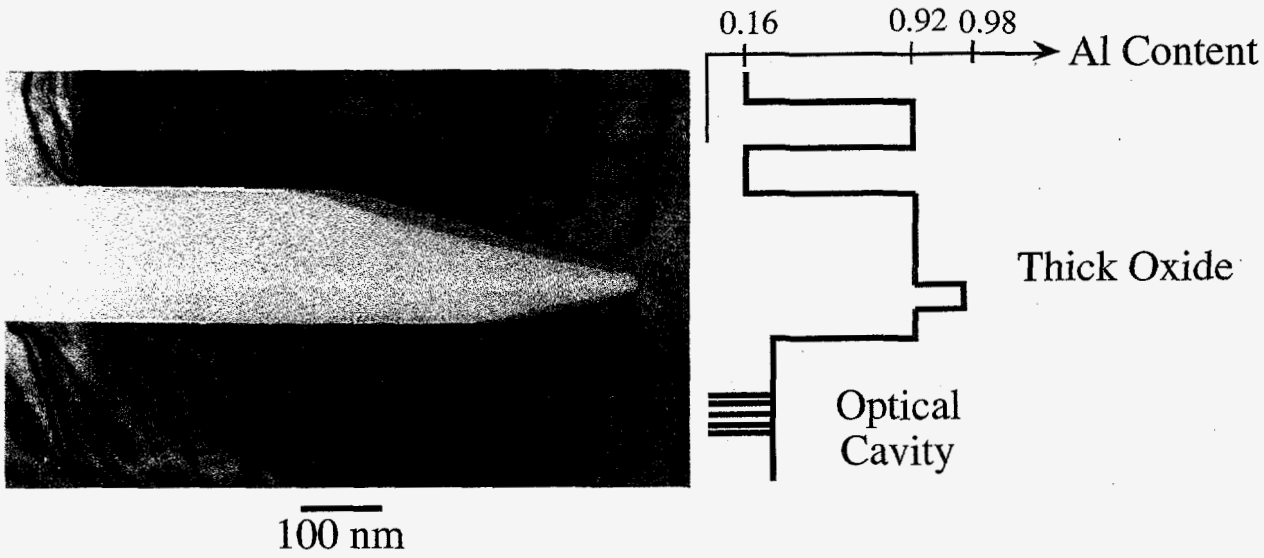

Figure 11. TEM image of thick tapered oxide.

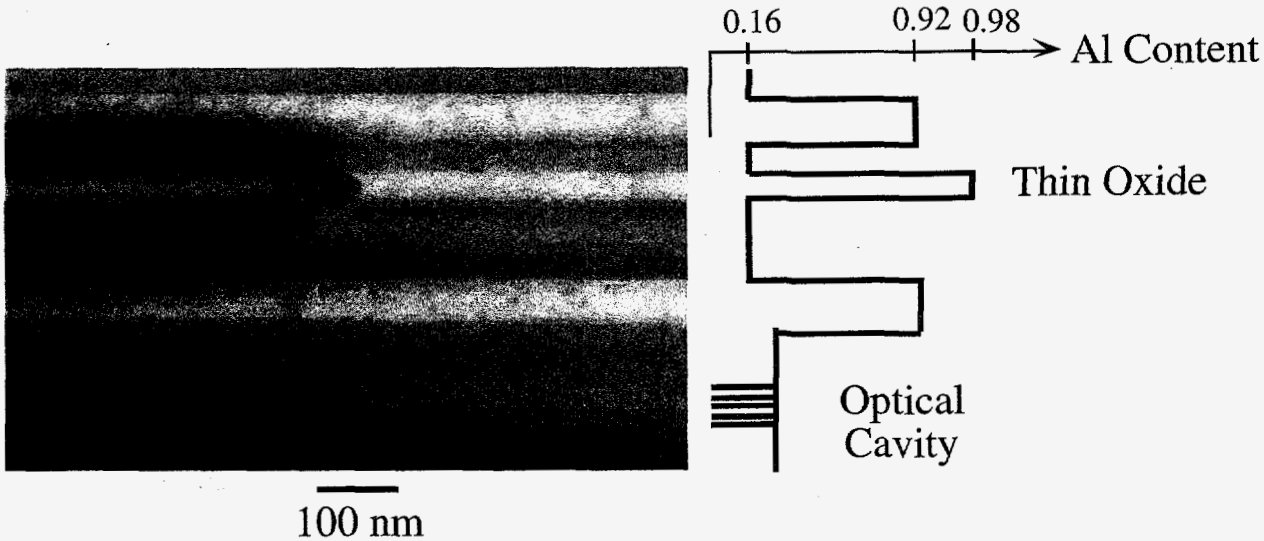

Figure 12. TEM image of thin oxide.

Fig. 11, a thin $Al_{0.98}Ga_{0.02}As$ layer is inserted at a field null between thicker $Al_{0.92}Ga_{0.08}As$ layers which compose the low index DBR layer. When this epitaxial structure is oxidized, a thick oxide with a tapered profile at its terminus is formed due to vertical oxidation into the $Al_{0.92}Ga_{0.08}As$ layers, where the taper tip corresponds to the position of the thin $Al_{0.98}Ga_{0.02}As$ layer. The more rapid lateral oxidation of the thin $Al_{0.98}Ga_{0.02}As$ layer "drags" along the oxidation of the thicker surrounding $Al_{0.92}Ga_{0.08}As$ layers. The result is the oxidation rate of the $Al_{0.98}Ga_{0.02}As$ ($Al_{0.92}Ga_{0.08}As$) layer is decreased (increased) by a factor of 1.5 (3.0) relative to a bulk layer. This produces the tapered oxide profile in the thick oxides apparent in Fig. 11. Similar thick oxide apertures with the taper tip positioned at the field antinode were also designed. Fig. 12 shows a thin

$Al_{0.98}Ga_{0.02}As$ layer placed at the field null within a high index 3/4-wavelength thick $Al_{0.16}Ga_{0.84}As$ layer. The lower Al composition of the surrounding layers of the low index DBR layer enforces a thinner oxide at the field null. In the following sections, we compare the optical confinement and modal characteristics arising from these oxide aperture designs.

3.1.2. Optical Confinement

We first consider the optical confinement arising from the thick oxides where the taper tip is positioned at a longitudinal field null (see Fig. 11) or antinode, or for the thin oxide at a longitudinal field null (see Fig. 12). In Figure 13 the optical mode width measured at 1.2 x threshold current using high magnification near-field beam profiling is plotted versus the oxide aperture size. For all structures, the lasers operation single mode below a specific device size. For the thick tapered oxides, the mode size monotonically decreases with decreasing aperture size, but the oxide tip positioned at the field null produces slightly larger mode size. For the thin oxide, the mode size is much larger, and in fact is greater than the aperture size for the smallest lasers. This behavior is consistent with the reduced optical confinement of oxide apertures which overlap field nulls, particularly as the optical mode width approaches the oxide aperture size. The greater mode size from the thin oxide VCSEL would seem to be advantageous for single mode output, but as we describe below, the accompanying modal discrimination must also be considered.

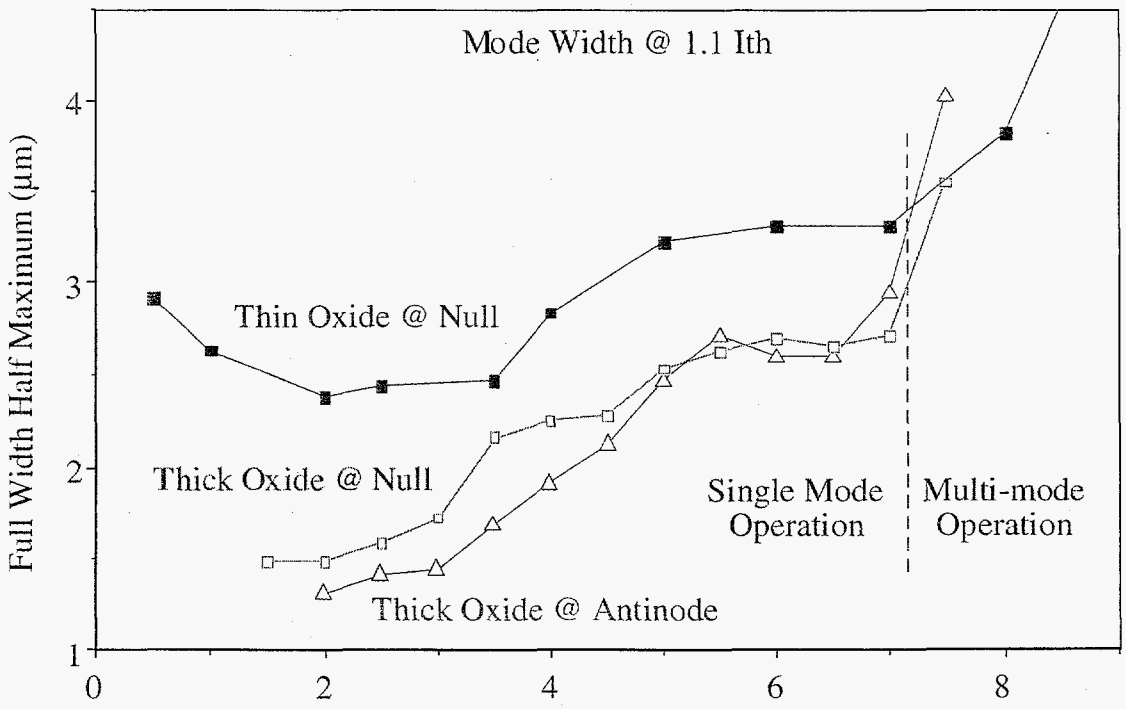

Figure 13. Near field mode width versus aperture size.

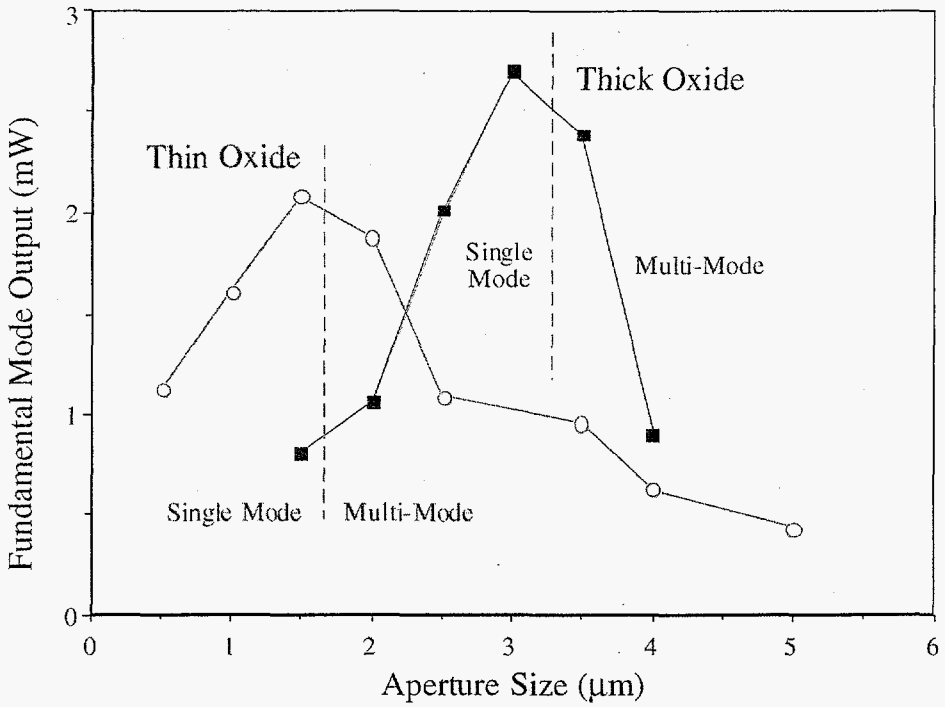

Figure 14. Maximum single mode power versus aperture size.

3.1.3. Single Mode Properties

Figure 14 is a plot of the maximum single mode output power obtained using the oxide designs shown in Figures 11 and 12. Note that above a particular aperture size, the VCSELs operate multimode. In this condition, the single mode output decreases, since the other modes can access the laser gain. The thick tapered oxide aperture VCSELs exhibit single transverse mode emission over a range of aperture cross section sizes, in contrast to previous observations of selectively oxidized VCSELs. The 182 nm thick transparent oxide aperture VCSELs depicted in Figure 11 possess a single transverse mode over their entire current operation for cross section area ≤ 3.5 x 3.5 μm. By contrast, multimode emission is obtained for all aperture sizes using a 84 nm (1/4-wavelength) thick oxide with an abrupt profile due to much greater optical confinement.

Notice the thin oxide VCSEL only operates single mode for apertures ≤ 1.5 x 1.5 μm. Even though the confinement of the fundamental mode has been reduced (due to the decreased overlap between the optical standing wave and the thin oxide), the modal discrimination of the higher order modes is also reduced. The thick tapered oxide produces greater modal discrimination, which allows the device to operate single mode at larger cavity diameters. The maximum single mode power from a selectively oxidized VCSEL was 3.5 mW, and used a thick tapered oxide such as shown in Figure 11.

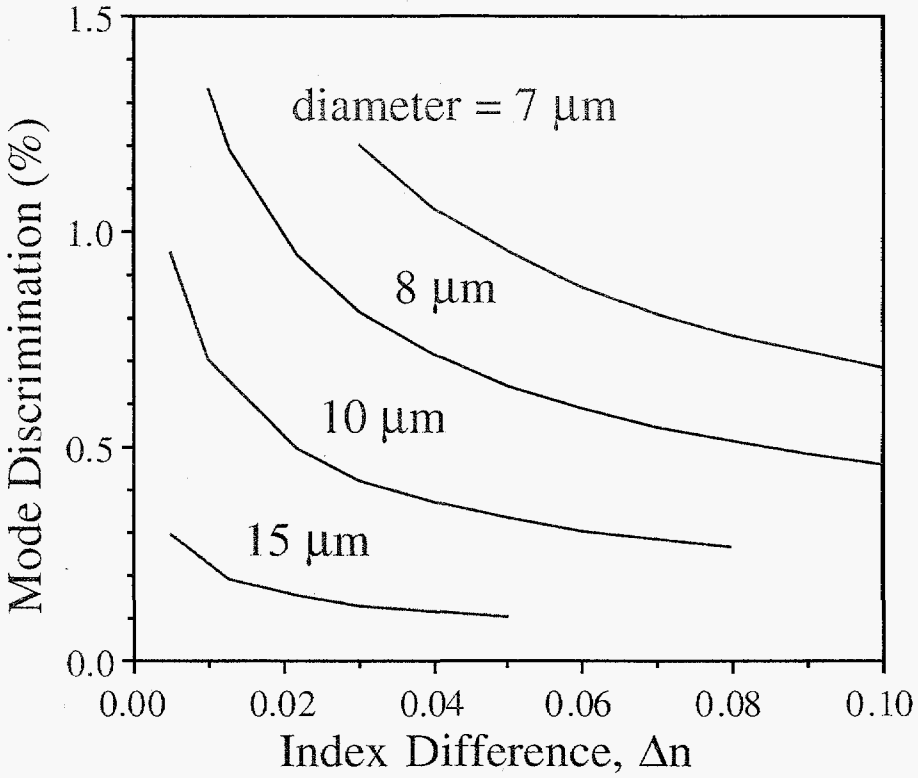

Figure 15. Design plot for leaky mode VCSELs.

3.2. Leaky Mode Designs

The spatial/spectral hole burning in implanted VCSELs and the strong index guiding inherent to etched air-post or selectively oxidized VCSELs inevitably produce multi-transverse mode operation. Leaky mode structures employing high refractive index regions surrounding the laser cavity to suppress high order optical modes can enable single mode operation in single element lasers and laser arrays. Prior leaky mode edge emitting and VCSEL device structures have relied upon lateral material variations to create the index profile necessary for leaky mode behavior. Recently R. Hadley has shown that modifications of the VCSEL longitudinal cavity resonance will effectively produce transverse index variations which can be used to engineer the transverse index profile.

An antiguided laser will have a high refractive index material surrounding a lower index laser cavity to produce greater loss for higher order modes due to greater extent outside of the cavity than the fundamental Gaussian mode. However, the loss of all transverse modes will increase with this index profile, so the design of an antiguided laser requires a balance between the excess loss of higher order modes relative to the fundamental mode loss. Shown in Fig. 15 is the calculated excess loss between the fundamental and first higher order mode of a VCSEL. For a small negative index step between the cavity and cladding

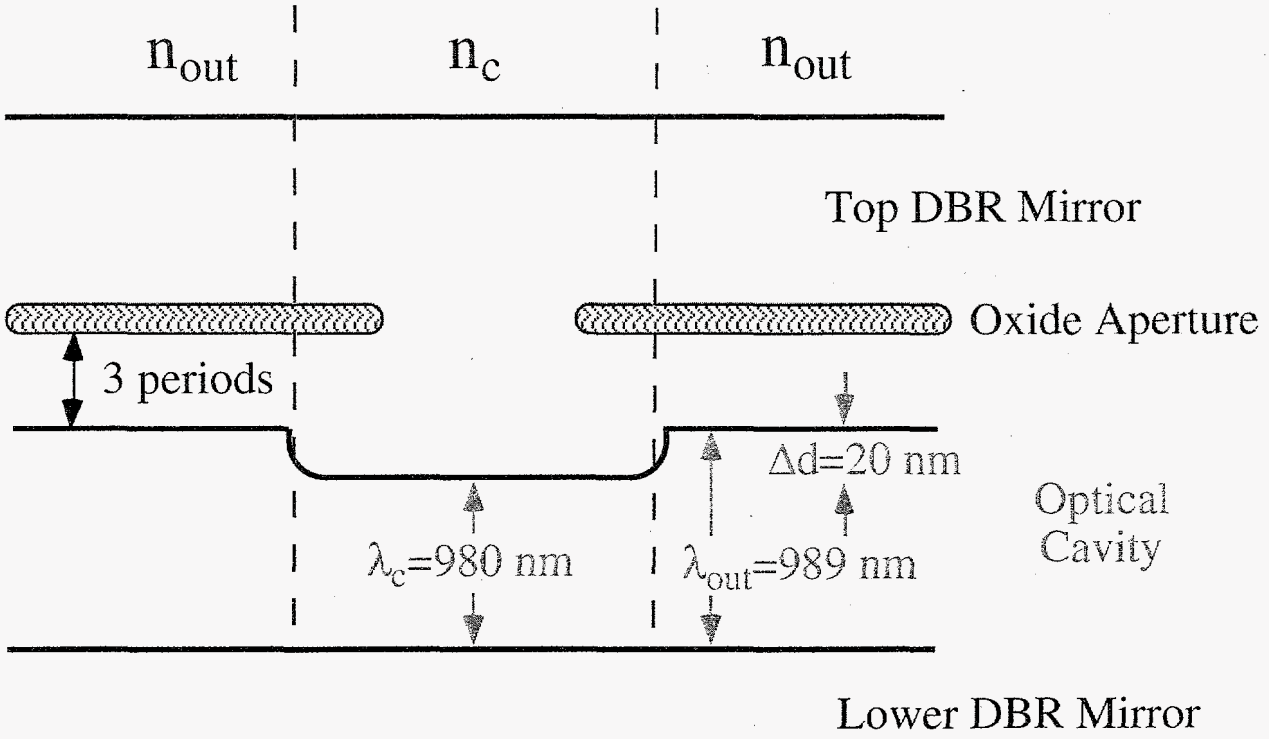

Figure 16. Sketch of leaky mode VCSEL utilizing transverse cavity resonance modification.

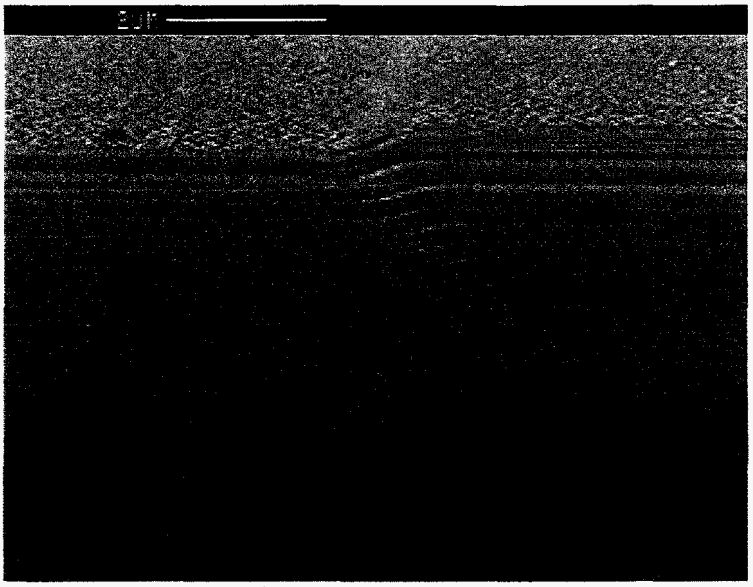

Figure 17. Scanning electron microscope image of leaky mode VCSEL. Notice the smooth overgrowth over the etched step.

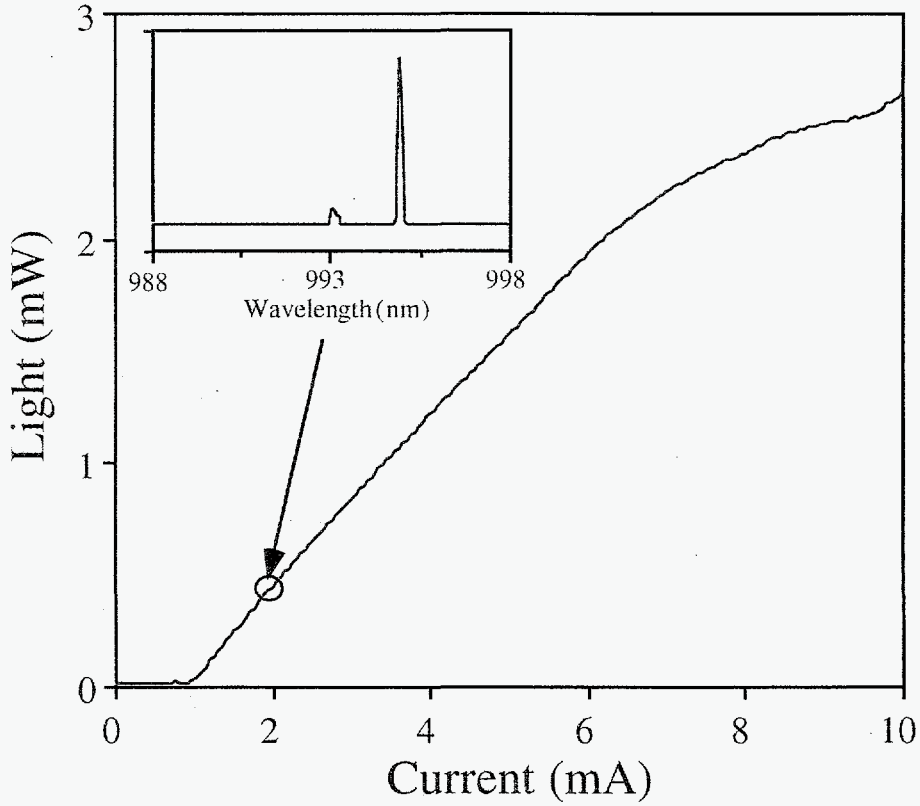

Figure 18. Light output and corresponding lasing spectrum (see inset) for VCSELs surrounded by d=30 nm longer cavity (Δn=0.055).

regions, Δn, the loss for all transverse modes and the excess loss plotted in Fig. 15 will increase due to the increased radiation loss. Large Δn leads to reduced excess modal loss and permits multi-mode behavior. At intermediate Δn values, high excess loss with simultaneous low fundamental mode loss can be achieved, which will discriminate against the higher order modes. The leaky mode VCSEL simulations predict good modal discrimination for 7 μm diameter lasers with an index step of Δn = 0.02-0.04.

To accomplish such a transverse index variation, an etch/regrowth fabrication process is used to laterally modify the VCSEL longitudinal cavity resonance. First, the bottom distributed Bragg reflector mirror and optical cavity for a nominally 980 nm VCSEL are grown by metalorganic vapor phase epitaxy. As shown in Fig. 16, an additional thickness, d, is added to the one wavelength thick optical cavity. Next, the sample is patterned and holes of varying diameter are dry etched to remove the excess material and thus define the laser cavity. A top semiconductor distributed Bragg reflector mirror is then overgrown as shown in Figure 17. Note the oxide aperture will induce index confinement (positive Δn) and thus is positioned away from the optical cavity to diminish its influence. Leaky mode VCSELs with various hole depths (and thus induced values of Δn) were fabricated to compare their modal characteristics.

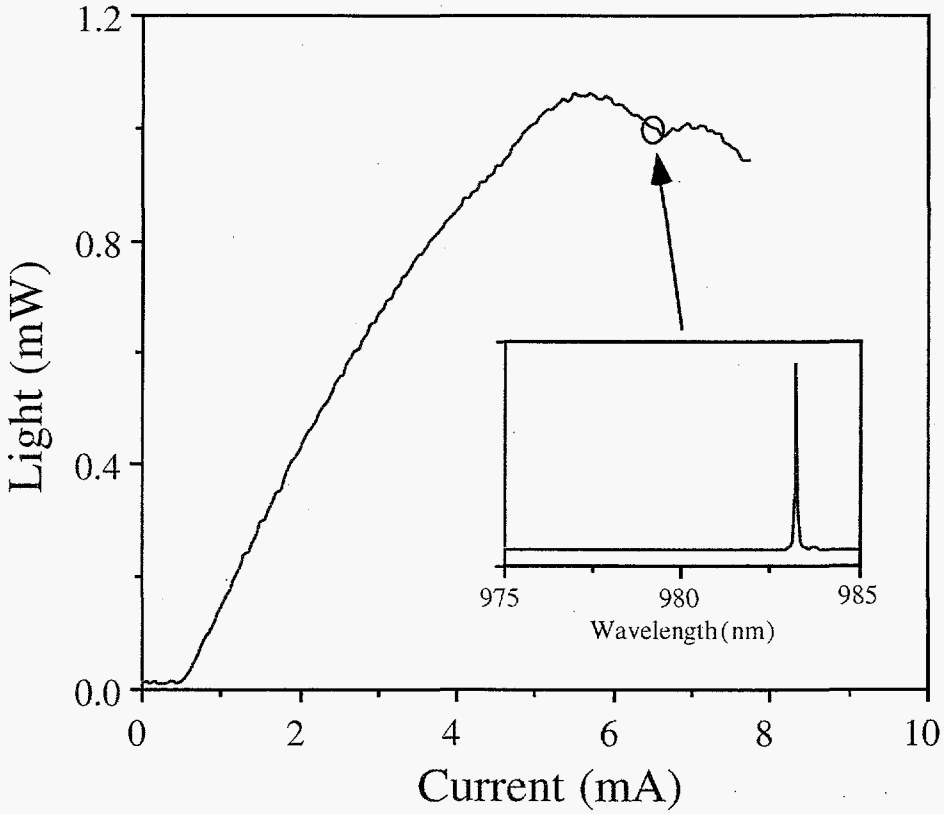

Figure 19. Light output and corresponding lasing spectrum (see inset) for antiguided VCSEL surrounded by d=20 nm longer cavity (Δn=0.03)

In Figures 18 and 19 are plotted the light output and spectral characteristics of two leaky mode etched/regrown VCSELs which have 7 μm diameter cavity diameter as defined by the etched hole, and approximately 5x5 μm oxide apertures. In Fig. 18 the VCSEL is surrounded by a 30 nm longer cavity which produces Δn=0.055; note this device exhibits multi-mode emission near threshold as shown in the inset. Multi-mode operation results from the reduced radiation loss and modal discrimination accompanying the higher Δn (see Fig. 15). The maximum single mode power from this VCSEL is < 0.5 mW. The relatively smooth light output curve and high maximum output power is a consequence of the good spatial overlap of the multiple transverse modes with the gain region. The higher threshold current in Fig. 18 is due to the spectral misalignment between resonance and laser gain because of the shorter cavity (deeper etched hole).

In Fig. 19 the leaky mode VCSEL is surrounded by a 20 nm longer cavity which yields Δn=0.03 as suggested from Fig. 15. This VCSEL exhibits a Gaussian near field profile and a single lasing emission spectrum up to injection currents >13 times the threshold current due to the reduced degree of antiguiding. The cavity resonance is at longer wavelength than in Fig. 18 and thus more closely matches the laser gain; however this gain/resonance alignment

will tend to promote higher order modes. The designed antiguiding in the VCSEL discriminates against the higher order modes producing > 1 mW of single mode power at rollover in Fig. 19, but lower maximum output power is obtained due to less efficient utilization of the laser gain.

In summary, leaky mode VCSELs employing cavity resonance modification to achieve antiguiding have been demonstrated. VCSELs with moderate values of antiguided fabricated by an etch/regrowth process have enabled single transverse mode emission to greater than 13 times threshold. Higher single mode output powers from individual VCSELs can be expected using optimized mirror and cavity designs. Furthermore, antiguided 2-dimensional arrays based on this technology appear promising for high power single mode applications.

4. Summary

We have developed VCSEL designs for achieving high output power, either multimode or single mode. For raw multimode output power, the output mirror reflectivity, dopant distribution, and laser cross section area all are important considerations. Under pulsed conditions, a broad area VCSEL has produced >1 W. Employing 2-dimensional VCSEL arrays allows scaling up the power also. We have demonstrated > 0.5 W under CW operation; pulsed VCSEL operation has not been explored.

For single mode operation, the transverse optical confinement must be modified. By using thick tapered oxides, we have increased the single mode output be discriminating against higher order transverse optical modes. Alternatively, by employing leaky mode structures, we have also demonstrated single mode operation to > 13 times threshold. The latter VCSELs were fabricated using a MOVPE regrowth technology. High power operation from VCSELs will enable emerging applications.

15	MS0603	Kent Choquette (1712)
1	MS9018	Central Technical Files (8940-2)
2	MS0899	Technical Library (4916)
1	MS0619	Review & Approval Desk (00111)
1	MS0188	LDRD Office (4001)